Brain Dynamics during Arousal-dependent Pleasant/Unpleasant Visual Elicitation: An Electroencephalographic Study on the Circumplex Model of Affect

Alberto Greco* *Member, IEEE*, Gaetano Valenza *Senior Member, IEEE*, and Enzo Pasquale Scilingo *Senior Member, IEEE*

Abstract—Emotion regulation to pleasant and unpleasant stimuli involves several brain areas, such as the prefrontal cortex, amygdala, and insular cortex. However, how a specific arousal level affects such brain dynamics is not fully understood. To this effect, we propose an electroencephalography (EEG)-based study, where 22 healthy subjects were emotionally elicited through affective pictures gathered from the International Affective Picture System. Based on the circumplex model of affect, we used four arousing levels, each with two valence levels (i.e. pleasant and unpleasant). Considering these levels, we investigated the EEG power spectra and functional connectivity among channels. We then used this information to build an automatic valence classifier.

The experimental results showed that the functional connectivity at the highest frequency bands (i.e. > 30Hz) was most sensitive to arousal modulation. Specifically, high connectivity over the right hemisphere occurred during pleasant elicitation, whereas that over the left hemisphere occurred during negative elicitation. In addition, short-range connections in the frontal regions became weaker with increased arousal level, whereas long-range connections were enhanced.

Concerning the spectral analysis, the most significant valence-dependent changes were found at intermediate arousing elicitations over the prefrontal and occipital regions. The automatic valence classification showed a recognition accuracy of up to 86.37%.

1 Introduction

Emotion regulation occurring at the central nervous system (CNS) level involves a complex interplay of cortical (e.g. frontal, temporal, and parietal) and subcortical (e.g. basal ganglia, thalamus, amygdala, and hippocampus) regions across a variety of both positive and negative emotions [1], [2]. Particularly, the limbic system includes or is highly interconnected to these regions and it is considered the primarily responsible for our emotional life [3]–[5]. One example concerns the amygdala and hippocampus, which subtly but importantly interact in emotional situations [6]. In fact, the amygdala can modulate both the encoding and the storage of hippocampal-dependent memories. The hippocampus, by forming episodic representations of the emotional significance and interpretation of events, can influence the amygdala response when emotional stimuli are encountered. The limbic system is strongly connected also with the nucleus accumbens, which plays a role in sexual arousal [7] and with the orbitofrontal cortex, the part of the prefrontal cortex that is thought to represent emotion and reward in decision making [8]. Another specialised prefrontal region that is regularly implicated in affective regulation is the anterior cingulate cortex (ACC) [9], which plays a relevant role in the cognitive control of emotion. The prefrontal cortex and the amygdala constitute the core of two specific pathways. Riuz-Padial et al. [10] suggested that briefly presented emotion stimuli access the fast route of emotion recognition perhaps via the amygdala. Instead, longer elicitations allow activating the prefrontal cortex that produces a context appropriate response.

Several models in the literature are used to describe emotions. A common approach attempts to classify emotions using a number of discrete "basic emotions", including happiness, fear, surprise, sadness, interest, rage, and disgust [11], [12]. On the other hand, many researchers agree that emotions have at least two important dimensions: valence (pleasantness) and arousal (low/high intensity of perception). Also theorists who mainly support basic discrete emotion theory find merit in the role of valence and arousal dimensions (e.g. [13], [14]). Some theorists emphasize one or the other as basic to affective experience (e.g. [15]–[17]. Instead, others incorporate both (e.g. [18]–[21]) pointing out how these two dimensions could be hierarchically related to discrete emotions [22]. One of the most widely used model of emotion, which follows the dimensional approach, is the circumplex model of affect (CMA) [21], [23], [24]. The CMA, proposes that all affective states arise from two fundamental neurophysiological systems, one related to valence and the other to arousal [19]. Each emotion can be understood as a linear combination of these two dimensions, or as varying degrees of both valence and arousal.

Consequently, arousal and valence are often considered to be independent. However, in a real-world experience, a certain degree of correlation between them can be easily observed (e.g., negative stimuli tend to evoke more intense and arousing perceptions than positive) [25]. Accordingly, some psychological studies have hypothesised a linear/nonlinear correlation between self-reported scores of valence and arousal [26]–[28]. To investigate the extent of this interdependence, previous research studied brain activity associated with affective stimuli. Particularly, recent fMRI studies [29], [30] aimed to decode the neural response

* *Corresponding Author: a.greco@centropiaggio.unipi.it.*
The authors are with the Research Center "E. Piaggio", School of Engineering, University of Pisa, Largo Lucio Lazzarino 1-56122, Pisa, Italy.

to chemosensory valence and arousal stimuli, showing that amygdala activity changes as a function of arousal intensity, but not of valence. Conversely, the activity of the orbitofrontal cortex activity changes with valence level, but not with the arousal. Similar results were also confirmed using affective words [25], however they found that those brain areas where activity was modulated by the interaction between arousal and valence, i.e. left medial orbitofrontal cortex and striatum.

Another approach to investigating CNS during emotion elicitation employs electroencephalographic (EEG) signals to locate cortical activation during emotional processing and regulation [31]–[33]. Previous findings showed a relationship between emotions and brain power spectral density (PSD) in EEG over the frontal cortex [34]–[36]. In fact, the EEG power spectra and functional connectivity in high frequency bands (e.g. β and γ bands) were found to be sensitive to valence changes [33], [33], [35], [37]–[40]. Also, increased gamma rhythms were associated with pleasant/unpleasant stimuli [41]–[44], along with enhanced activity in the beta band over the temporal and parietal areas during negative tasks [45].
Asymmetry and lateralization of brain activity have also been implied in emotional processing [35], [46]–[48]. Although controversial [35], previous evidence suggests the existence of asymmetric brain activity patterns associated with specific emotional states [49] (e.g. evidence of the right hemisphere's contribution to sexual arousal).

The aforementioned quantitative and functional EEG analyses were often exploited for the development of automatic emotion recognition [50]–[53], [53], [54], [54]. However, to the best of our knowledge, previous EEG-based affective computing methods considered valence and arousal along independent axes [50]–[52], while disregarding a possible interaction-effect that might influence recognition accuracy [55], [56]. In fact, previous evidence supports a nonlinear interaction-effect between arousal and valence perception [25], [27], [28].

Therefore, in this study we investigate changes in EEG spectra and functional connectivity evoked by pleasant and unpleasant visual elicitation as a function of different arousal levels. Preliminary findings of this research were recently reported in [56], [57]. In addition, we propose a pattern recognition algorithm that predicts the valence level of a stimulus as a function of the arousal level.

2 Materials and Methods

2.1 Experimental paradigm and acquisition set-up

Twenty-two healthy volunteers (in the age range of $21-24$ years) signed an informed consent to participate in our experiment. Each participant was asked to answer a Patient Health Questionnaire^{TM} (PHQ-9). The PHQ-9 is a multiple-choice self-report questionnaire that is commonly used to screen and diagnose mental health disorders, e.g., depression. We enrolled in the study only those volunteers with a score below a threshold of 5, to have a homogeneous sample of healthy subjects [58]. In fact, PHQ-9 test indicates the possibility of a mild depression for scores greater than 5 [58]–[60]. All experimental procedure were previously

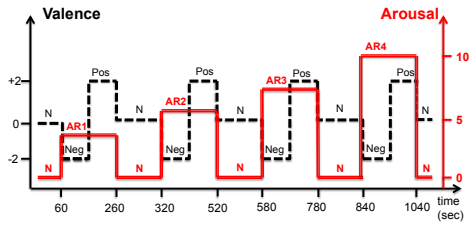

Figure 1. Exemplary timeline of the experimental protocol. The red line represents the arousal level of the stimulation throughout the experiment, whereas the black dashed line an exemplary valence level. The order of the positive and negative sub-sessions was randomised among subjects.

approved by the Ethical Committee of the University of Pisa-Pisa University Hospital, Pisa (Italy).

To design our experiment, we relied on the CMA that represents emotions in a multi-dimensional plane [21], whose two principal dimensions are *valence* and *arousal*. *Valence* indicates the degree of pleasantness, whereas *arousal* could be interpreted as the intensity of the affective perception. According to the previous literature, a typical and effective way to evoke pleasant and unpleasant emotions consists in the presentation of affective slides [61]. One of the most widely used datasets of affective pictures is the International Affective Picture System (IAPS) [62]. It is a frequently cited tool in the field of affective computing and has been often used also in EEG studies [63]–[65]. IAPS collects more than 900 pictures each of which is associated with an arousal and valence score averaged over more than a thousand subjects.

Accordingly, we selected a set of pictures from the IAPS database and we split it in 5 groups based on their arousal levels (see Table 1): *neutral* (N) and *arousal* 1–4 (AR1,AR2, AR3, AR4). The experimental timeline was structured in 9 sessions alternating each of the four *arousal* session between two *neutral* sessions (N) as shown in Figure 1. Each *arousal* session was considered comprised of two sub-sessions according to the valence level. More in detail, each sub-session included ten IAPS images with positive valence (pleasant) and ten with negative valence (unpleasant). The images were visualised onto a PC screen for 10 s each. Moreover, to reduce the effects of external factors (such as time), the order of positive and negative sub-sessions was randomised among subjects.

Throughout the experiment, EEG signals were recorded by means of the Geodesic EEG Systems 300 from the Electrical Geodesics, Inc. Such a device is characterised by its comfort and the ease of cuff use . The Geodesic cuff included 128 electrodes. However, we only considered herein the data acquired from 19 electrodes placed on the scalp according to the International Standard System 10-20, specifically, Fp1,

Table 1
Arousal Rating of the IAPS Images Used

Session	Arousal rating	Arousal range	Arousal level
N	2.81 ± 0.24	$2.42 - 3.22$	VL
A1	3.58 ± 0.30	$3.08 - 3.98$	L
A2	4.60 ± 0.31	$4.00 - 4.99$	L-M
A3	5.55 ± 0.28	$5.01 - 6.21$	M-H
A4	6.50 ± 0.33	$5.78 - 6.99$	H

Fp2, F7, F3, Fz, F4, F8, T7, C3, C4, T8, P7, P3, Pz, P4, P8, O1, O2, and Oz. The sampling frequency was set at 1 KHz. The mastoid signal average was used as a reference. The experiment was performed in strictly controlled conditions. The room was illuminated by a white neon lighting, with a power of 50 lumens, equally distributed. Subjects were asked to sit on a comfortable chair at a fixed distance of 70 cm from a screen configured with maximum brightness.

2.2 EEG pre-processing

The raw EEG recordings were processed using MATLAB and the EEGLAB toolbox [66]. First, we implemented an efficient pre-processing scheme to discard corrupted and noisy data, made up of the following stages: data filtering, head/body movement artefact detection and removal, eye blink artefact detection and removal and interpolation of corrupted channels. Afterwards, we computed a spectral and functional connectivity analysis.

2.2.1 Data filtering

The out-of-band noise that affected the raw EEG data were reduced applying a 6^{th}-order bandpass infinite impulse response filter with a passband from 1 to 45 Hz.

2.2.2 Head/body detection and removal

The EEG signals of all channels were divided into 4s epochs and their amplitude distribution was calculated. Afterwards, we cautiously excluded the epochs above the 95th percentile due to possible contamination related to head and/or the body movement artefacts [67]. As a validation of this automatic process we performed also a further visual inspection.

2.2.3 Eye artefacts detection and removal

To detect possible eye blink artefacts, we calculated sliding-window cross-correlation to estimate time-varying correlations between the frontal electrodes and the electrooculogram. Values above a specific threshold, calculated using phase-randomised surrogated data [68], suggested the presence of possible eye artefacts. When these fluctuations above the correlation threshold lasted more than 70 ms and coincided with an amplitude of the frontal EEG channels above 50μV they were definitely considered as ocular artefacts. Also in this case, the epochs containing such artifacts were eliminated after a further visual inspection [69].

2.2.4 Interpolation of corrupted channels

In case of corrupted channels, EEG signals show a high-frequency noise and several unexpected events [66]. To detect EEG-corrupted channels, we considered a 3D-space whose axes were the second, third, and forth central moments. The good EEG channels were commonly clustered together, whereas the corrupted ones drifted apart in different directions according to their artefactual nature [67]. Outliers (i.e., values whose distance from the cluster centroid was greater than twice the interquartile range for at least one dimension) were identified as corrupted channels and, after confirmation through visual inspection, replaced with interpolated data. Of note, among the 19 selected channels of all subjects only the 1.67 % of them were replaced.

2.3 Spectral Analysis

An EEG spectral analysis was performed to calculate the power spectral density (PSD) of each time-series, considering the classical frequency bands: θ [4−8 Hz), α [8−14 Hz), β [14−32 Hz) and γ ($\geq$ 32 Hz) [67]. PSD was estimated through Welch's method [70] averaging the power spectra calculated in moving time windows of 4 s with 75% (3 s) of overlap aiming at decreasing the PSD variance.

2.4 EEG functional connectivity analysis

The functional connectivity analysis was performed measuring the phase synchronization for each pair of channels in each frequency band using the mean phase coherence index (MPC) [71].

$$R^2 = E[cos(\Delta\phi)]^2 + E[sin(\Delta\phi)]^2 \quad (1)$$

Where R represents the MPC; $\Delta\phi$ is the relative phase difference between two channels derived by the instantaneous difference of the analytic signals from the Hilbert transform, and E is the expectation operator. MPC values can oscillate between 0 and 1. The MPC is close to 1 when a strong phase synchronization exists between two channels. Alternatively, MPC is close to 0 if the two channels are not synchronised.

2.5 Statistical analysis and classification procedure

For both the power spectrum and MPC values of each electrode we assessed statistical differences between the pleasant and unpleasant sub-sessions. More in detail, we used a non parametric Wilcoxon test for paired samples [72] with Holm–Bonferroni-correction for multiple testing. A non-parametric test was necessary due to the non-gaussianity of the data as ascertained by the Kolmogorov-Smirnov test ($p < 0.05$).

In addition, as regards the functional connectivity analysis, we performed also a Friedman test for each electrode pair to study the differences of the MPC values among the four positive and four negative arousal sub-sessions We also performed two separate analyses for the two valence levels. Each Friedman p-value correspondent to each electrode pair reported if there was, at least, one significant change among the four positive and four negative arousal sub-sessions. Moreover, a post-hoc test using the Bonferroni adjustment was conducted to investigate all the pairwise comparisons among the four arousal sub-sessions.

Finally, we implemented a classification procedure to automatically identify the positive and negative valence stimuli. We considered sixteen different input datasets in order to analyze the effect of the four arousal levels and four EEG bands on the recognition accuracy. For each dataset, to reduce the risk of overfitting, the dimension of the feature space was reduced through an unbiased dimensionality reduction strategy. More in detail, the power estimated within each EEG band and each arousal level (i.e. sixteen feature sets) were taken as input of a KNN classifier, which was validated through a leave-one-subject-out (LOSO) cross validation. Specifically, each training set comprised data from $(N-1)$ subjects, where N is the total number of participants, and was used to recognize the emotional valence of the N_{th} left-out subject. This procedure was iterated N times.

KNN has been chosen because it is one of the most popular algorithms for pattern recognition. It is a simple supervised memory-based algorithm, and makes no hypothesis about the distribution of its free parameters, while requiring no model to be fitted [73]. Many researchers demonstrated that the KNN classifier achieves very good performance on different applications [74]–[77]. Furthermore, the rationale that underlies the KNN leads to alleviate the curse of dimensionality by reducing the less significant dimensions of the feature space [78]. Of note, a disadvantage concerns the computation requirement, which is not relevant for this study.

As mentioned before, within the LOSO scheme, we applied a dimensionality reduction process for each input dataset, considering only the electrodes that showed a significant difference between the positive and negative stimuli in the training set. Alternatively, the principal component analysis (PCA) is applied to the training set and the two principal components were selected in case no electrodes showed significant differences. The PCA transformation matrix is then applied to the test set.

Moreover, the input data matrix was transformed in a within-subject rank matrix based on the Friedman statistical test, i.e., the feature vectors from a given subject were transformed into ranks. More specifically, the examples relative to a single subject for each feature were transformed in ranks. Fig. 2 shows a block diagram of the proposed recognition system.

The accuracy results of the validation process are presented in the manuscript through confusion matrices [79]. The percentage value in the cell c_{ij} represents the rate of how many observations of the class i are classified as belonging to class j. Accordingly, matrices with high values along the diagonal show a highly accurate classification output.

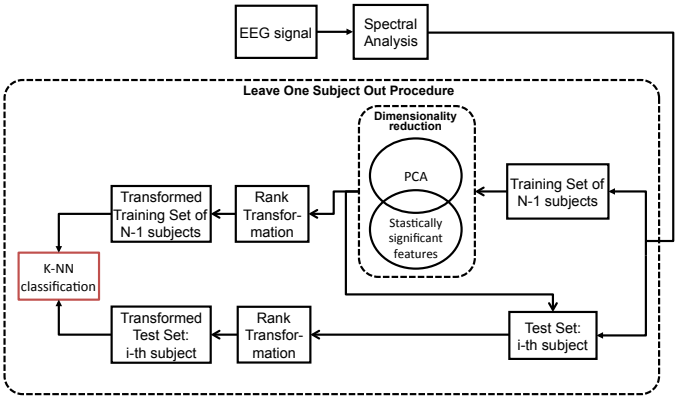

Figure 2. Overall block scheme of the proposed arousal and valence recognition system. The EEG is processed to extract the spectral components using the Welch algorithm. According to the protocol timeline, the spectral results are statistically compared and transformed in within-subject rank matrices after a dimension reduction procedure, applied on at each iteration, on the training set. The KNN classifier was engaged to perform the pattern recognition by adopting a leave-one-subject-out procedure.

3 Experimental Results

3.1 Statistical results

3.1.1 Spectral statistical results

Results from statistical analysis between pleasant and unpleasant stimuli on spectral quantifiers are shown in Fig. 3 as p-value topographic maps. Each column in the figure represents one of the four arousing elicitation session (from AR1 to AR4). Red (blue) areas indicate a significant increase (decrease) in PSD during the pleasant elicitation with respect to the negative one. Green areas indicate no statistical difference. Statistical correction for multiple testing was also applied according to the Holm–Bonferroni [72] procedure.

Focusing on the θ bandwidth, the lowest and highest arousal levels did not present any significant differences between the positive and negative IAPS stimuli. Instead, the analysis of the L-M arousal level (AR2) showed a greater activity during the positive elicitation than the negative one in the frontal midline area. The occipital right area was more activated by the negative images. As regards the M–H arousal level (AR3), a slightly significant increase of the PSD could be seen in the frontal left region during the positive valence stimuli.

The α band results showed that we obtained a diametrically opposite behaviour compared to all the other bandwidths. In this case, the statistically significant differences between the two valence levels only occurred during the highest and lowest arousal levels of stimulation. The PSD significantly increased in the parietal midline area during the negative stimuli when the subjects watched the images at the lowest arousal level. Meanwhile, an increase of the negative PSD was shown in the parietal left region for the highest arousal stimuli.

The valence comparison in the β band showed an increase in the frontal right area during the positive stimuli at arousal 1. The negative stimuli caused a greater activation of the frontal left area compared to the positive ones when the arousal level was increased during the AR2 stimulation. This highly activated area, which was related to the negative stimulation, migrated and spread to the fronto-polar, frontal midline and temporal right areas at the AR3 level. The highest level of arousal stimulation for θ showed no significant difference between the two valence levels.

Results in the γ band showed no significant differences between positive and negative elicitation during AR1 session. Instead, throughout AR2 a strong increase was noted both in the parietal-occipital lobes and in the frontal midline and fronto-polar left regions. The trend of spectral differences in AR2 reversed in AR3. In fact, the frontal left area (around the F3 electrode) significantly increased its activity during the negative elicitation wrt the positive one. Likewise, also the occipital right region activity increase during the unpleasant sub-session. Finally, the differences between the two valence levels were totally suppressed when the arousal reached the highest level.

3.1.2 Functional connectivity statistical results

As regards the functional connectivity, we report in Fig. 4 and 5 the results of the two proposed analyses.
Concerning the PSD, Fig. 4 shows, for each arousal level,

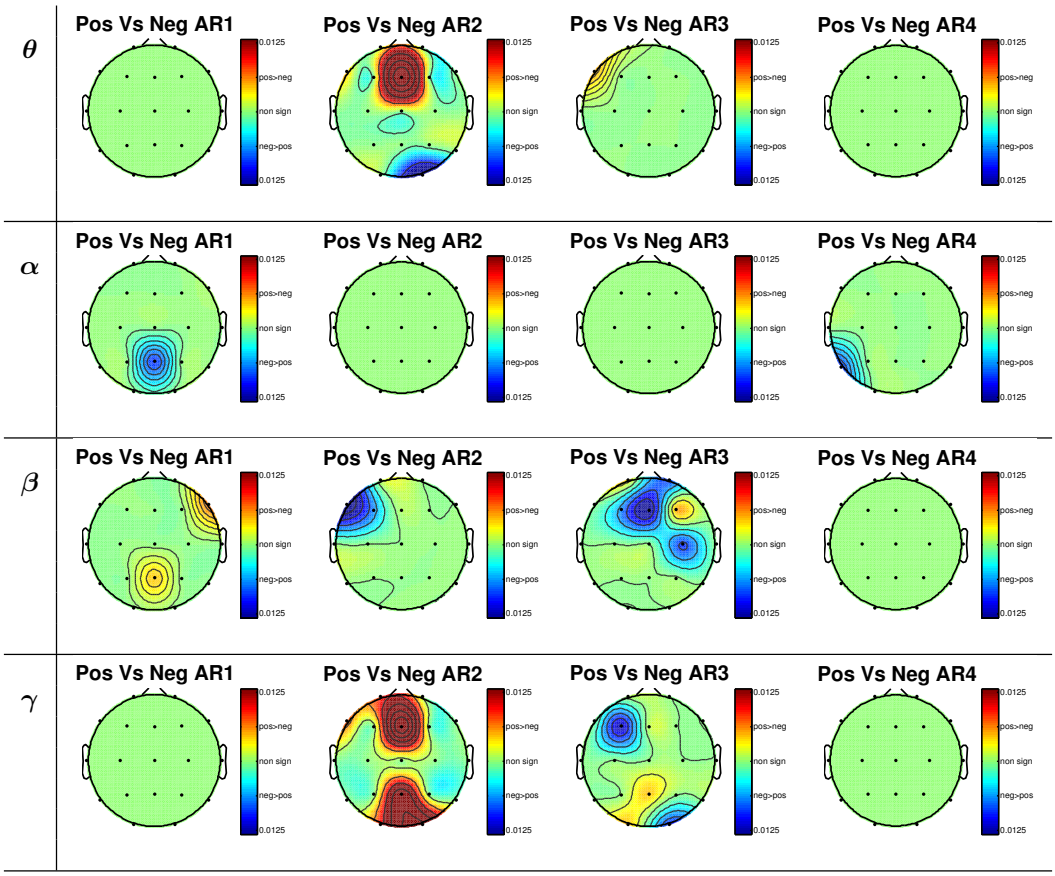

Figure 3. P-value maps resulting from the statistical analysis on EEG-PSD estimated from positive (Pos) and negative (Neg) sub-sessions of each arousal session (AR1–AR4). Each row represent a different frequency band: θ (top), α (middle-top), β (middle-bottom) and γ (bottom) band.

functional connections that were significantly different between pleasant and unpleasant sub-sessions. Red arrows are associated with a significant increase of the MPC during the positive valence sub-sessions in comparison with the negative ones. Meanwhile, the blue arrows indicate a significant greater activation associated with a negative elicitation as compared to the positive one.
At the lowest level of arousal (i.e., AR1), for all bandwidths, we found significant connections associated with both positive and negative stimuli. Instead, concerning the intermediate arousal levels, i.e., AR2 and AR3, the negative stimuli increased functional connections at the lowest frequencies (i.e., δ and α), whereas the positive stimuli increased the MPC computed at the highest bandwidths (i.e., β and γ). Of note, the AR3 session analysed in γ band was an exception as no statistically significant variations were found. As regards the highest arousal level (i.e., AR4), most of the significant connections were associated with negative stimuli. Note that the number of significantly synchronised electrodes strongly decreased for α, β and γ bands.

Fig. 5 reports the significant changes on the MPC values among all the positive and negative sub-sessions at different arousal levels. The Friedman test was performed to show if there was at least one difference among all the arousal levels. The related post-hoc test with the Bonferroni correction highlighted which pair of arousal levels determined the significant increase or decrease of the MPC value. The MPC "increase" in the text below referred to the red arrows that represent a consistent increase with the arousal level increase. On the contrary, "decrease" referred to the blue arrows that represent a decrease of the MPC value in contrast with an increase in the arousal level.

Among the pleasant arousing stimulations in θ band (Figure 5-A, first line), the significant changes were related with the connections between the left and right hemispheres, specifically on the frontal, temporal, central, and parietal regions. Other significant differences occurred between the parietal midline and occipital electrodes. The latter significantly changed, and the MPC of the T7–F4 and Cz–P8 pairs of electrodes decreased when the arousal level increased. Instead, the MPC of Fp1-C4, F4-P3, and F4-P4 coherently increased when comparing AR1/AR2 and AR4. We obtained a strong increase of the MPC index on the unpleasant elicitations (Figure 5-A, second line), which was consistent with the arousal level between the extreme right and left frontal electrodes, when comparing AR2 to AR4. A significant stronger connection was also shown between C4 and P8. The short-range connections Fp2-Fz, Fp2-Cz and P7-O1 were significantly weaker at an increasing arousal level.

The Friedman test showed a small number of significant differences between the positive and negative valences considering the results in the α band (Figure 5-B). Among the positive stimuli, the post-hoc analysis showed a MPC decrease for the short-range connections between Fp2-Fz, F4-F8 and Pz-O1. Meanwhile, we found a stronger connection between the temporal left and parietal right regions (T7–

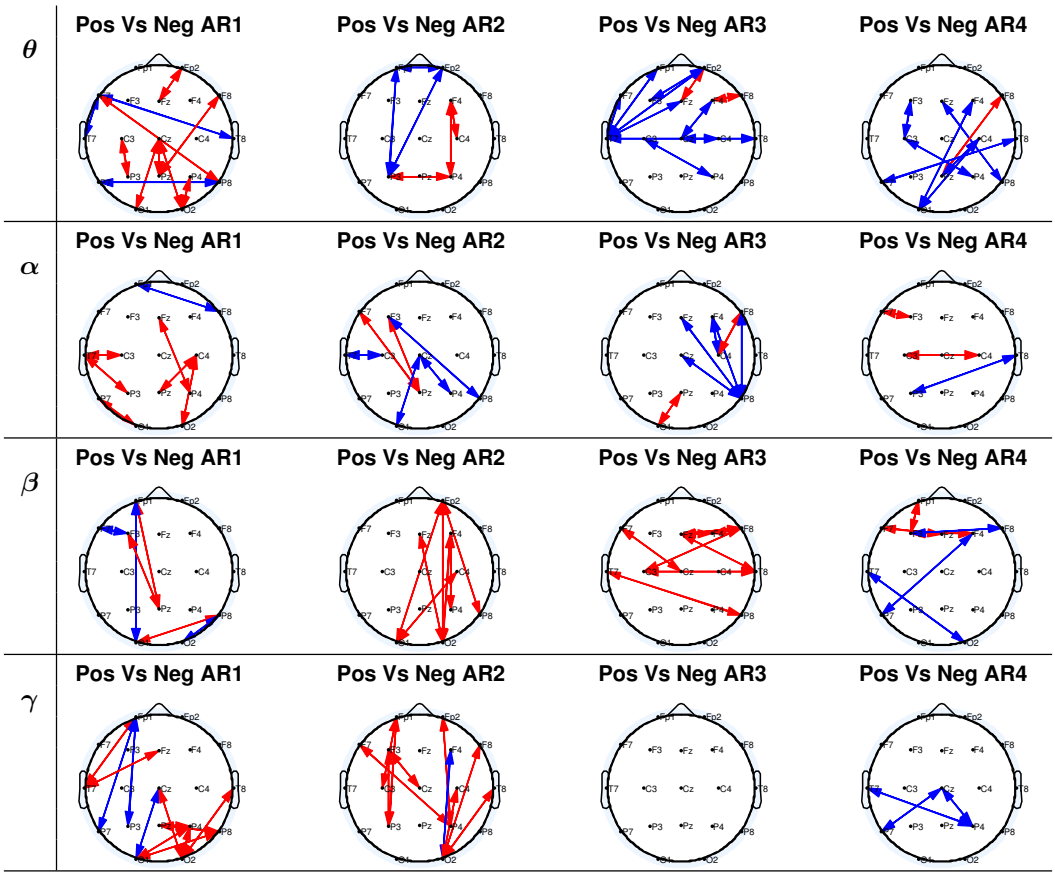

Figure 4. P-value maps resulting from the statistical analysis on MPC estimated from positive (Pos) and negative (Neg) sub-sessions of each arousal session (AR1–AR4). Each row represent a different frequency band: θ (top), α (middle-top), β (middle-bottom) and γ (bottom) band. Red arrows represent a significant increase in the positive sub-sessions in comparison with the negative sub-sessions. Conversely blue arrows represent a significant increase in the negative sub-sessions.

P4), between the frontal right and left (F3–F4), and frontal midline and central right areas (Fz–C4) during arousal 4. As regards the negative stimulation, the arousal increase only produced two significant MPC decreases between Fp1–Fz (comparing AR1 vs AR2) and C3–O1 (comparing AR1 vs AR3).

The number of significant changes greatly increased for the higher frequencies. The Friedman test showed many significant changes in the electrode synchronization on the whole scalp considering the β band (Figure 5-C). On the one hand, the positive stimuli showed a higher concentration of arrows around the midline region and the temporal and parietal right areas. On the other hand, the negative stimuli showed such in the frontal left area. The highest arousal level for the positive valence strengthened the synchronizations between the frontal and the parietal areas. In addition, the MPC decreased with the arousal increase from AR1 to AR3 and AR4 for the fronto-polar and the occipital electrodes. A comparison of AR1 and the higher arousal levels showed a general suppression of the connections between the frontal and fronto-polar areas for negative stimulation. Meanwhile, a comparison of AR3 with both AR1 and AR2 demonstrated that observing a significantly stronger connection between the temporal left and right electrodes was possible. Compared with AR1 and AR2, other stronger connections were found at level AR4 for the electrode pairs Fz-Cz, Fz-C4, Fp1-P4, T7-P7 and Cz-P7.

The Friedman test showed that most of the significant changes among different arousal levels on the pleasant elicitations in the γ band (Figure 5-D) involved short-range connections between the electrodes in the right hemisphere and both within and between the frontal, parietal, central, and occipital areas. However, long synchronizations between Fp2–P4 and F8–O2 were also found. Most of the significant variations in the negative arousal sessions were in the left hemisphere, especially in the left frontal channel (F7). The post-hoc analysis showed that the negative elicitation brought about weaker connections, except for F7–P3, when the arousal level was increased. On the contrary, a majority of significant changes, specifically in the central and frontal areas, were consistent with the increase of the arousal level, considering the pleasant stimuli.

3.2 Classification results

Tables 2, 3, 4, and 5 show the classification procedure results on the four groups of datasets corresponding to different arousal levels. The recognition accuracy was reported in the form of a confusion matrix as follows: the closer the elements on the main diagonal are to 100%, the higher the degree of the recognition accuracy.

We performed four different classifications of the two valence levels for each arousal level, separately considering each of the four bandwidths.

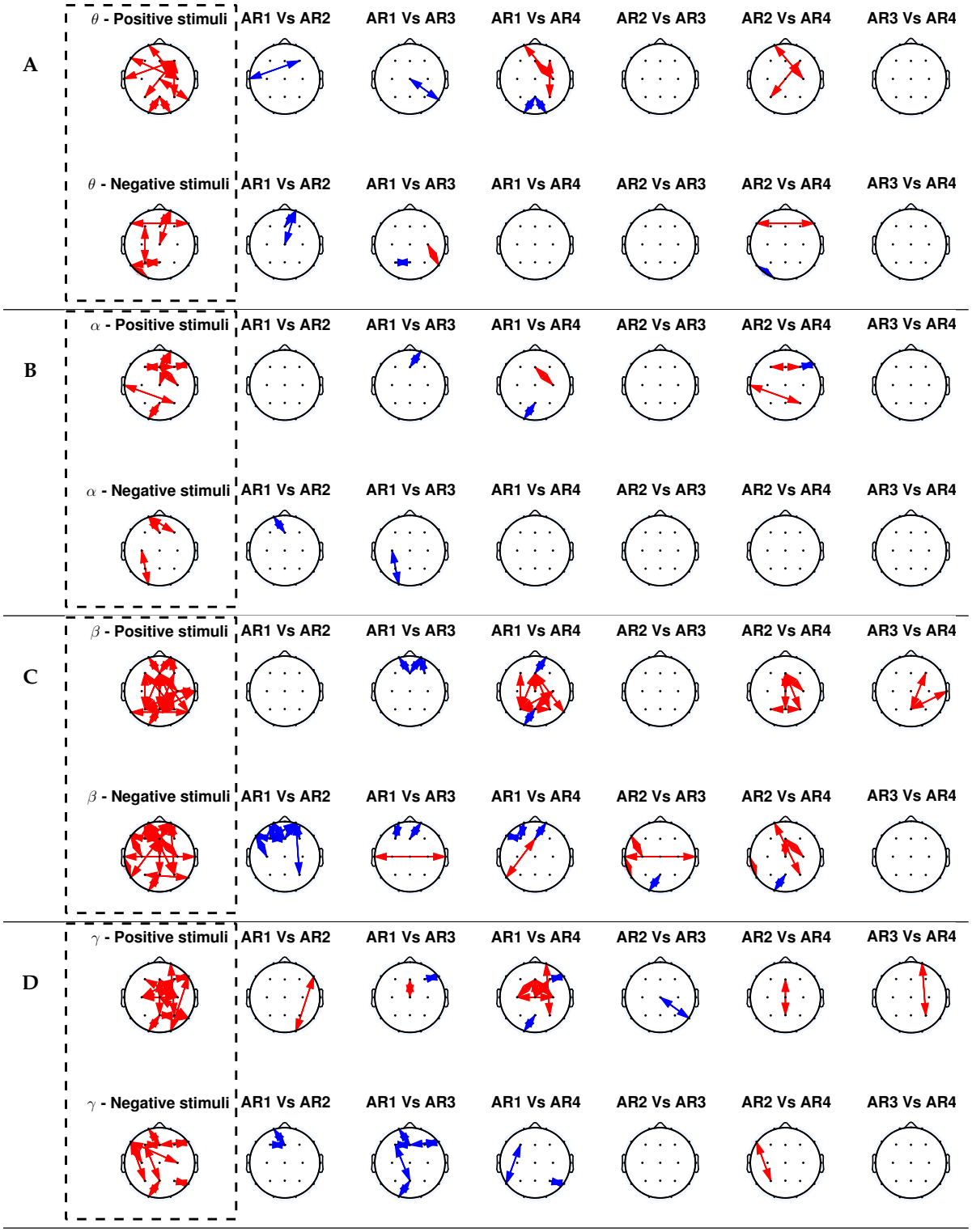

Figure 5. Significant changes of the MPC in all bands (p-value < 0.05) between the electrodes in the positive (up) and negative (bottom) sub-sessions. For each sub-figure, the two topographic maps on the left framed by a dotted line represent the Friedman significant results. The other twelve maps (six for each valence level) show the post-hoc analysis results for all pairs of arousal levels. The blue arrows in the post-hoc analysis maps represent a significant increase of the MPC in sessions with a lower arousal level. The red arrows represent a significant increase in the session with a greater arousal level. The results are calculated in the θ (A), α (B), β (C) and γ (D) bands.

Table 2
Confusion matrix of the positive vs the negative valence classification considering the arousal 1 level and each bandwidth feature set.

KNN	Band	Positive valence	Negative valence
Positive valence	θ	86.36 %	90.91%
	α	**77.27%**	27.27%
	β	**72.73%**	27.27%
	γ	54.55%	54.55%
Negative valence	θ	13.64%	9.09%
	α	22.73%	**72.73%**
	β	27.27%	**72.73%**
	γ	45.45%	45.45%

Table 3
Confusion matrix of the positive vs the negative valence classification considering the arousal 2 level and each bandwidth feature set.

KNN	Band	Positive valence	Negative valence
Positive valence	θ	**77.27 %**	27.27%
	α	68.18 %	59.09%
	β	**81.82%**	18.18%
	γ	**86.36%**	18.18%
Negative valence	θ	22.73%	**72.73%**
	α	31.82%	40.91%
	β	18.18%	**81.82%**
	γ	13.64%	**81.82%**

Table 4
Confusion matrix of the positive vs the negative valence classification considering the arousal 3 level and each bandwidth feature set.

KNN	Band	Positive valence	Negative valence
Positive valence	θ	**72.73 %**	22.73%
	α	50.00%	50.00%
	β	**90.91%**	18.18%
	γ	**86.36%**	18.18%
Negative valence	θ	27.27%	**77.27%**
	α	50.00%	50.00%
	β	9.09%	**81.82%**
	γ	13.64%	**81.82%**

Considering the data from the lowest level of arousal stimulation (AR1), the spectral features were able to recognise the two valence levels with an average accuracy for each band equal to θ=47.72%, α=75% and β=72.73% γ=50% (Table 2).
The average accuracies for all the bandwidths improved considering AR2 and AR3, except for the α band. The classification procedure showed an average accuracy of θ=75.00%, α=54.55%, β=81.82% and γ= 84.09%, for the arousal 2 datasets (Table 3) and an even better accuracy considering the arousal 3 level: θ=75.00%, α=50%, β=86.37% and γ= 84.09% (Table 4). The arousal 4 datasets showed a strong decrease of the average accuracy as follows: θ=47.73%, α=68.18%, β=56.82%, γ= 50.00% (see Table 5).

Table 5
Confusion matrix of the positive vs the negative valence classification considering the arousal 4 level and each bandwidth feature set.

KNN	Band	Positive valence	Negative valence
Positive valence	θ	81.82%	86.36%
	α	**68.18%**	31.82%
	β	45.45%	31.82%
	γ	68.18%	68.18%
Negative valence	θ	18.18%	13.64%
	α	31.82%	**68.18%**
	β	54.55%	68.18%
	γ	31.82%	31.82%

4 Discussion and Conclusion

We investigated the interaction effect between the arousal and valence perceptions on brain dynamics during a visual affective elicitation. To this end, we performed a spectral and functional connectivity analyses on EEG signals from 22 healthy volunteers and using the spectral results to implement an automatic pattern recognition system. The experimental protocol comprised four arousing sessions at an increasing intensity, where the valence levels changed from unpleasant to pleasant or vice-versa, randomly. Affective visual stimuli were chosen in terms of arousal and valence from the IAPS database. The PSD and the MPC were computed within four classical frequency bandwidths (i.e. θ [4−8 Hz), α [8−14 Hz), β [14−32 Hz) and γ ($\geq$ 32 Hz)) after a proper pre-processing. Differently from previous studies, which commonly considered valence and arousal along independent axes or combine their values to recognize discrete emotional states [80], we studied changes in brain dynamics evoked by pleasant and unpleasant stimuli as a function of different arousal levels.

Among the multitude of parametric and nonparametric measures quantifying brain functional connectivity, we applied the MPC index, which demonstrated good effectiveness in EEG studies [71], [81], [82]. The statistical analysis on the MPC results was performed to study the differences in synchronization dynamics between two electrodes after positive and negative stimulation at group-wise level. This method [83] allows for gathering reliable results, less affected by measure-specific parameters and to highlight what we can define as statistical significant functional connectivity variations.

Functional connectivity may not underlie anatomical connection, and yet its very definition has proved to be problematic [84]. In its most general sense, functional connectivity refers to synchronous patterns in the firing of different neuronal assemblies. There is no unique interpretation of short- and long-range connectivity. For example, in [85] and [86], they found that long-range networks preferably oscillate at low frequencies, whereas short-range connectivity is reflected by α or γ waves [87]. However, the possibility that α oscillations may play an important role for long-range connectivity under different types of cognitive demands is still open [88]. In this study, θ and α EEG oscillations comprised short- and long-range functional connectivity whose magnitude increased during unpleasant emotional elicitation than a positive one (see Fig. 4). On the other hand, β and γ EEG oscillations comprised short- and long-range functional connectivity whose magnitude increases during pleasant emotional elicitation than a negative one. In addition, we provided evidence that, both in the case of pleasant and unpleasant stimuli, increasing of arousing levels affected short- and long-range functional connectivity especially in the higher frequencies, i.e., β and γ bands. Significant changes involving posterior association cortices and between the left dorsolateral prefrontal cortex and posterior regions were found especially after negative

stimuli of different arousing levels (see Fig. 5). Different arousal levels of positive stimuli, instead, affected changes of short- and long-range functional connections in the right hemisphere.

Moreover, the results showed that the short-range connections involving the frontal and parietal-occipital areas generally became weaker with the increasing arousal for both positive and negative elicitations. In contrast, the long-range connections were strengthened by the high arousal pleasant and unpleasant stimuli, specifically between the right and left hemispheres in the frontal and temporal regions and between the parietal and frontal electrodes.

Therefore, the emphasis of long-range connections as well as the suppression of short-range ones in the frontal and parieto-occipital areas are a phenomenon related to an increase of the arousal level for both positive and negative stimulations. Moreover, the brain hemisphere, where the changes in the MPC index occurred, may distinguish between pleasant and unpleasant stimuli for high frequency oscillations.

The spectral analysis results of the two valence levels were statistically analysed within each arousal session bandwidth. For each bandwidth, four topographic maps of p values related to each arousal level specifically showed significant changes between the pleasant and unpleasant stimulations.

Focusing on the alpha oscillations (8–14 Hz), a significant increase of the PSD occurred during the negative stimuli in the parietal-midline at the AR1 level and in the parietal right electrode at the AR4 level. No significant differences were found between the valence levels at AR2 and AR3. These results were in contrast with those related to other bands. The results for all the other bands indeed revealed the absence of a few significant changes between pleasant and unpleasant elicitations when the lowest and highest arousing levels occurred (i.e. AR1 and AR4). Meanwhile, the valence level changes during the intermediate arousal sessions (i.e. AR2 and AR3) were associated with significant variations in the activation of the prefrontal and parieto-occipital regions.

A greater activation of the frontal midline area in θ and γ, as well as a higher PSD in the parieto-occipital region for the γ oscillations were related to a positive stimulation during the AR2 session (i.e. low–medium arousal sessions). Considering a further higher arousal elicitation (AR3), an increase of the power activity of the frontal left area in γ and around the frontal midline and central right regions in β were the indices of an unpleasant stimulation. The perceived valence changes in arousing sessions 2–3 were associated with the significant changes in the prefrontal and parieto-occipital regions [34]. The frontal cortex was often associated with brain emotion processing driven by inputs from the brain's limbic system. In this case, the low–medium arousal stimuli favoured the activation of the frontal cortex in response to pleasant stimulation, whereas the high–medium arousal stimuli favoured the activation in response to an unpleasant one. Focusing on θ band, previous studies showed how synchronization increases upon presentation of "emotional" rather than "neutral" stimuli, highlighting a significant role of the temporal, parietal and prefrontal cortex [89], [90]. In agreement with these results, we found that a significant role was played by the frontal and parietal areas for low-medium arousing stimuli and in the temporal cortex for medium and high arousing stimuli. Indeed, negative stimuli increased synchronizations between the prefrontal and parietal cortex during AR2 session and over the temporal lobe during AR3 and AR4 sessions. These latter results may be in line with [89], in which θ synchronization activity reflected differential involvement of the left and right anterior temporal regions in the discrimination between positive and negative affective valences. Moreover, we found that an increasing of the arousal level from AR3 to AR4 was associated with the significant connectivity path due to the negative stimuli switching from the left to the right temporal cortex.

Pleasantness and unpleasantness perception produce a lateralized activation of the cortex power, although the current literature reports controversial findings. There are evidences supporting the hypothesis that pleasant stimuli induces an increased EEG activity over the left hemisphere with respect to the right hemisphere and conversely [91], [92]. On the other hand, recent studies reported a relatively increased power for unpleasant stimuli over the left temporal region with respect to the right and a general laterality shift towards the right hemisphere for positive emotional stimuli [93]. Other findings suggest also that positive and negative emotional stimuli involves the same areas as in the left hemisphere, regardless of the sensory modality [94]. In addition, a summary meta-analyses on 65 neuroimaging studies of emotion [95] found no evidence about the overall right-lateralization of emotional function, and limited evidence for valence-specific lateralization of emotional activity [95]. Accordingly, our results did not show a strong coherent lateralization of valence perception between the EEG power and arousal levels, confirming the difficulty in supporting one specific hypothesis.

The results of the spectral analysis were also used as the input of an automatic recognition algorithm. Also in this case, the accuracy of the classification varied depending on the bandwidth and the arousal level. The best accuracy was found considering the middle arousal levels. Moreover, the valence recognition was more accurate considering the highest frequency bandwidths, i.e. β (86.37%) and γ (84.09%). Indeed, the γ ($\geq$ 32 Hz) frequency bandwidth was considered in the literature as the valence-related band [33], [41]. Our results were in agreement with a possible non-linear relation between the CMA dimensions as found in different experimental protocols [25]. Particularly, according to the valence U-shape theory [25], our results suggested that with very high arousing stimuli, the central response to both positive and negative stimulation did not differ in terms of PSD as opposed to intermediate arousal.

Of note, results on the γ band could be affected by possible electromyogenic (EMG) contamination. Previous studies showed that even for electrodes located at a relative distance from the cranial muscles, the normal resting EEG shows significant contamination with EMG activity [96], [97]. Moreover, filtering as well as ICA-based methods could not be effective for this kind of artefacts [97]. In order to reduce this possible contamination, the experiment was performed in extremely strict controlled cnditions. The subjects were comfortably seated with a neck support, and

the dedicated channels of the Geodesic system to monitor the electromyographic signal. In addition, our analysis focused on differences between two emotional conditions. Assuming the possible EMG contamination as a background in the high frequency spectra, this *differential* analysis should further reduce the effect of EMG artefact on our results.

The present study was limited due to the fixed session sequences that could confound the arousal perception (especially for the first and forth levels) and, consequently, also the arousal-valence interaction. However, being our analyses focused on discriminating between positive and negative stimulation, the randomization of valence subsessions reduced the effect induced by the order of stimulus presentation. To further mitigate this limitation, a neutral session was used to separate the arousal blocks and bring the subject back to the baseline condition.

In summary, we investigated the role of valence perception in modulating brain dynamics across different arousal levels. To this end, we studied EEG power spectra and functional connectivity during visual emotional elicitation. Results show that emotional stimuli at intermediate arousing level affect brain dynamics in the γ band, especially in the frontal area, being particularly driven by positive stimuli at arousal level 2 and by negative ones at arousal level 3. This switching mechanism needs to be further investigated in future endeavours aimed to uncover cortical correlates of valence perception in humans. On the other hand, no significant differences were found between pleasant and unpleasant stimuli at the lowest and highest arousing levels. At a speculation level, the AR1 negative and positive images were possibly not arousing enough to be processed in an "affective way". Instead, the cortical affective processes at a very high arousal level (i.e. over a certain threshold; in this case, over AR3 level) were frozen because of the flood of emotional responses, which might mask underlying differences in cortical affective processes. Note also that, despite some limitations related to the stimuli presentation order along the arousal dimension, our results are in agreement with previous evidences linking brain dynamics and emotional valence [98]. In conclusion, our results raise concerns on the CMA regarding the valence and arousal dimension orthogonality, which is often assumed a-priori. Future works will be forward on the prediction of SAM scores regressing out EEG-derived metrics, as well as to the investigation of the role of gender in emotional processing.

REFERENCES

[1] J. C. Borod, *The neuropsychology of emotion*. Oxford University Press New York, 2000.

[2] R. D. Lane and L. Nadel, *Cognitive neuroscience of emotion*. Oxford University Press, USA, 2002.

[3] E. Fox, *Emotion science cognitive and neuroscientific approaches to understanding human emotions*. Palgrave Macmillan, 2008.

[4] J. E. LeDoux, "Emotion circuits in the brain," *Annual review of neuroscience*, vol. 23, no. 1, pp. 155–184, 2000.

[5] A. D. Craig and A. Craig, "How do you feel–now? the anterior insula and human awareness." *Nature reviews neuroscience*, vol. 10, no. 1, 2009.

[6] E. A. Phelps, "Human emotion and memory: interactions of the amygdala and hippocampal complex," *Current opinion in neurobiology*, vol. 14, no. 2, pp. 198–202, 2004.

[7] I. Aharon, N. Etcoff, D. Ariely, C. F. Chabris, E. O'Connor, and H. C. Breiter, "Beautiful faces have variable reward value: fmri and behavioral evidence," *Neuron*, vol. 32, no. 3, pp. 537–551, 2001.

[8] A. Bechara, H. Damasio, and A. R. Damasio, "Emotion, decision making and the orbitofrontal cortex," *Cerebral cortex*, vol. 10, no. 3, pp. 295–307, 2000.

[9] S. B. Perlman and K. A. Pelphrey, "Regulatory brain development: balancing emotion and cognition," *Social Neuroscience*, vol. 5, no. 5-6, pp. 533–542, 2010.

[10] E. Ruiz-Padial, J. Vila, and J. F. Thayer, "The effect of conscious and non-conscious presentation of biologically relevant emotion pictures on emotion modulated startle and phasic heart rate," *International Journal of Psychophysiology*, vol. 79, no. 3, pp. 341–346, 2011.

[11] P. Ekman, "Expression and the nature of emotion," *Approaches to emotion*, vol. 3, pp. 19–344, 1984.

[12] C. E. Izard, *Human emotions*. Springer Science & Business Media, 2013.

[13] I. J. Roseman, M. S. Spindel, and P. E. Jose, "Appraisals of emotion-eliciting events," *Journal of Personality and Social Psychology*, vol. 59, no. 5, pp. 899–915, 1990.

[14] C. A. Smith and P. C. Ellsworth, "Patterns of cognitive appraisal in emotion." *Journal of personality and social psychology*, vol. 48, no. 4, p. 813, 1985.

[15] E. Duffy, "An explanation of emotional phenomena without the use of the concept emotion," *The Journal of General Psychology*, vol. 25, no. 2, pp. 283–293, 1941.

[16] R. S. Lazarus, *Emotion and adaptation*. Oxford University Press on Demand, 1991.

[17] A. Ortony, G. L. Clore, and A. Collins, *The cognitive structure of emotions*. Cambridge university press, 1990.

[18] H. Schlosberg, "The description of facial expressions in terms of two dimensions," *Journal of experimental psychology*, vol. 44, no. 4, pp. 229–237, 1952.

[19] J. A. Russell, "A circumplex model of affect." *Journal of personality and social psychology*, vol. 39, no. 6, p. 1161, 1980.

[20] R. J. Larsen and E. Diener, "Promises and problems with the circumplex model of emotion." 1992.

[21] J. Posner, J. A. Russell, and B. S. Peterson, "The circumplex model of affect: An integrative approach to affective neuroscience, cognitive development, and psychopathology," *Development and psychopathology*, vol. 17, no. 03, pp. 715–734, 2005.

[22] J. A. Russell and L. F. Barrett, "Core affect, prototypical emotional episodes, and other things called emotion: dissecting the elephant." *Journal of personality and social psychology*, vol. 76, no. 5, p. 805, 1999.

[23] N. A. Remington, L. R. Fabrigar, and P. S. Visser, "Reexamining the circumplex model of affect." *Journal of personality and social psychology*, vol. 79, no. 2, p. 286, 2000.

[24] J. A. Russell, "Affective space is bipolar." *Journal of personality and social psychology*, vol. 37, no. 3, p. 345, 1979.

[25] P. A. Lewis, H. Critchley, P. Rotshtein, and R. Dolan, "Neural correlates of processing valence and arousal in affective words," *Cerebral cortex*, vol. 17, no. 3, pp. 742–748, 2006.

[26] P. J. Lang, M. K. Greenwald, M. M. Bradley, and A. O. Hamm, "Looking at pictures: Affective, facial, visceral, and behavioral reactions," *Psychophysiology*, vol. 30, no. 3, pp. 261–273, 1993.

[27] J. Winston, J. O'doherty, and R. Dolan, "Common and distinct neural responses during direct and incidental processing of multiple facial emotions," *Neuroimage*, vol. 20, no. 1, pp. 84–97, 2003.

[28] J. S. Winston, J. A. Gottfried, J. M. Kilner, and R. J. Dolan, "Integrated neural representations of odor intensity and affective valence in human amygdala," *Journal of Neuroscience*, vol. 25, no. 39, pp. 8903–8907, 2005.

[29] A. K. Anderson, K. Christoff, I. Stappen, D. Panitz, D. Ghahremani, G. Glover, J. D. Gabrieli, and N. Sobel, "Dissociated neural representations of intensity and valence in human olfaction," *Nature neuroscience*, vol. 6, no. 2, p. 196, 2003.

[30] D. M. Small, M. D. Gregory, Y. E. Mak, D. Gitelman, M. M. Mesulam, and T. Parrish, "Dissociation of neural representation of intensity and affective valuation in human gustation," *Neuron*, vol. 39, no. 4, pp. 701–711, 2003.

[31] R. Calvo, S. D'Mello *et al.*, "Affect detection: An interdisciplinary review of models, methods, and their applications," *Affective Computing, IEEE Transactions on*, vol. 1, no. 1, pp. 18–37, 2010.

[32] L. Sebastiani, A. Simoni, A. Gemignani, B. Ghelarducci, and E. Santarcangelo, "Autonomic and eeg correlates of emotional imagery in subjects with different hypnotic susceptibility," *Brain research bulletin*, vol. 60, no. 1, pp. 151–160, 2003.

[33] N. Martini *et al.*, "The dynamics of eeg gamma responses to unpleasant visual stimuli: From local activity to functional connectivity," *NeuroImage*, vol. 60, no. 2, pp. 922–932, 2012.

[34] J. A. Coan and J. J. Allen, "Frontal eeg asymmetry as a moderator and mediator of emotion," *Biological psychology*, vol. 67, no. 1, pp. 7–50, 2004.

[35] M. M. Müller, A. Keil, T. Gruber, and T. Elbert, "Processing of affective pictures modulates right-hemispheric gamma band eeg activity," *Clinical Neurophysiology*, vol. 110, no. 11, pp. 1913–1920, 1999.

[36] G. Vecchiato *et al.*, "How to measure cerebral correlates of emotions in marketing relevant tasks," *Cognitive Computation*, vol. 6, no. 4, pp. 856–871, 2014.

[37] M. J. Kim, R. A. Loucks, A. L. Palmer, A. C. Brown, K. M. Solomon, A. N. Marchante, and P. J. Whalen, "The structural and functional connectivity of the amygdala: from normal emotion to pathological anxiety," *Behavioural brain research*, vol. 223, no. 2, pp. 403–410, 2011.

[38] G. Varotto, P. Fazio, D. R. Sebastiano, G. Avanzini, S. Franceschetti, and F. Panzica, "Music and emotion: An eeg connectivity study in patients with disorders of consciousness," in *Engineering in Medicine and Biology Society (EMBC), 2012 Annual International Conference of the IEEE*. IEEE, 2012, pp. 5206–5209.

[39] A. A. Fingelkurts, A. A. Fingelkurts, H. Rytsälä, K. Suominen, E. Isometsä, and S. Kähkönen, "Impaired functional connectivity at eeg alpha and theta frequency bands in major depression," *Human brain mapping*, vol. 28, no. 3, pp. 247–261, 2007.

[40] M. Chen, J. Han, L. Guo, J. Wang, and I. Patras, "Identifying valence and arousal levels via connectivity between eeg channels," in *Affective Computing and Intelligent Interaction (ACII), 2015 International Conference on*. IEEE, 2015, pp. 63–69.

[41] C. S. Herrmann, A. Mecklinger, and E. Pfeifer, "Gamma responses and erps in a visual classification task," *Clinical Neurophysiology*, vol. 110, no. 4, pp. 636–642, 1999.

[42] B. Güntekin and E. Basar, "Emotional face expressions are differentiated with brain oscillations," *International Journal of Psychophysiology*, vol. 64, no. 1, pp. 91–100, 2007.

[43] H. J. Yoon and S. Y. Chung, "Eeg spectral analysis in valence and arousal dimensions of emotion," in *Control, Automation and Systems, 2011 11th International Conference on*. IEEE, 2011, pp. 1319–1322.

[44] J. A. Onton and S. Makeig, "High-frequency broadband modulation of electroencephalographic spectra," *Frontiers in human neuroscience*, vol. 3, p. 61, 2009.

[45] W. J. Ray and H. W. Cole, "Eeg alpha activity reflects attentional demands, and beta activity reflects emotional and cognitive processes," *Science*, vol. 228, no. 4700, pp. 750–752, 1985.

[46] R. J. Davidson, "11 affect, cognition, and hemispheric specialization," *Emotions, cognition, and behavior*, p. 320, 1984.

[47] J. C. Borod, B. A. Cicero, L. K. Obler, J. Welkowitz, H. M. Erhan, C. Santschi, I. S. Grunwald, R. M. Agosti, and J. R. Whalen, "Right hemisphere emotional perception: Evidence across multiple channels," *NEUROPSYCHOLOGY-NEW YORK-*, vol. 12, pp. 446–458, 1998.

[48] F. C. Murphy, I. Nimmo-Smith, and A. D. Lawrence, "Functional neuroanatomy of emotions: a meta-analysis," *Cognitive, Affective, & Behavioral Neuroscience*, vol. 3, no. 3, pp. 207–233, 2003.

[49] D. M. Tucker and S. L. Dawson, "Asymmetric eeg changes as method actors generated emotions," *Biological Psychology*, vol. 19, no. 1, pp. 63–75, 1984.

[50] Y.-P. Lin, C.-H. Wang, T.-L. Wu, S.-K. Jeng, and J.-H. Chen, "Eeg-based emotion recognition in music listening: A comparison of schemes for multiclass support vector machine," in *Acoustics, Speech and Signal Processing, 2009. ICASSP 2009. IEEE International Conference on*. IEEE, 2009, pp. 489–492.

[51] G. Chanel, J. Kronegg, D. Grandjean, and T. Pun, "Emotion assessment: Arousal evaluation using EEG and peripheral physiological signals," in *International workshop on multimedia content representation, classification and security*. Springer, 2006, pp. 530–537.

[52] A. E. Hassanien, M. Kilany, E. H. Houssein, and H. AlQaheri, "Intelligent human emotion recognition based on elephant herding optimization tuned support vector regression," *Biomedical Signal Processing and Control*, vol. 45, pp. 182–191, 2018.

[53] T. F. Bastos-Filho, A. Ferreira, A. C. Atencio, S. Arjunan, and D. Kumar, "Evaluation of feature extraction techniques in emotional state recognition," in *Intelligent human computer interaction (IHCI), 2012 4th international conference on*. IEEE, 2012, pp. 1–6.

[54] O. Sourina, Y. Liu, and M. K. Nguyen, "Real-time EEG-based emotion recognition for music therapy," *Journal on Multimodal User Interfaces*, vol. 5, no. 1-2, pp. 27–35, 2012.

[55] J. Li, Z. Zhang, and H. He, "Hierarchical convolutional neural networks for eeg-based emotion recognition," *Cognitive Computation*, pp. 1–13, 2017.

[56] A. Greco, G. Valenza, and E. P. Scilingo, "Valence-dependent changes in visual arousing elicitation: An exploratory study in eeg gamma oscillations," in *Engineering in Medicine and Biology Society (EMBC), 2016 IEEE 38th Annual International Conference of the*. IEEE, 2016, pp. 4555–4558.

[57] G. Valenza, A. Greco, A. Lanata, C. Gentili, D. Menicucci, L. Sebastiani, A. Gemignani, and E. P. Scilingo, "Brain dynamics during emotion elicitation in healthy subjects: An eeg study," in *AEIT International Annual Conference (AEIT), 2015*. IEEE, 2015, pp. 1–3.

[58] K. Kroenke, R. L. Spitzer, and J. B. Williams, "The phq-9," *Journal of general internal medicine*, vol. 16, no. 9, pp. 606–613, 2001.

[59] A. Coulter, V. A. Entwistle, A. Eccles, S. Ryan, S. Shepperd, and R. Perera, "Personalised care planning for adults with chronic or long-term health conditions," in *Cochrane Database of Systematic Reviews*, A. Coulter, Ed. Chichester, UK: John Wiley & Sons, Ltd, mar 2015.

[60] R. S. Shim, P. Baltrus, J. Ye, and G. Rust, "Prevalence, treatment, and control of depressive symptoms in the united states: results from the national health and nutrition examination survey (nhanes), 2005–2008," *The Journal of the American Board of Family Medicine*, vol. 24, no. 1, pp. 33–38, 2011.

[61] R. D. Lane, E. M. Reiman, M. M. Bradley, P. J. Lang, G. L. Ahern, R. J. Davidson, and G. E. Schwartz, "Neuroanatomical correlates of pleasant and unpleasant emotion," *Neuropsychologia*, vol. 35, no. 11, pp. 1437–1444, 1997.

[62] P. J. Lang, M. M. Bradley, and B. N. Cuthbert, "International affective picture system (iaps): Affective ratings of pictures and instruction manual," *Technical report A-8*, 2008.

[63] M. R. Lemke, C. J. Fischer, T. Wendorff, G. Fritzer, Z. Rupp, and S. Tetzlaff, "Modulation of involuntary and voluntary behavior following emotional stimuli in healthy subjects," *Progress in Neuro-Psychopharmacology and Biological Psychiatry*, vol. 29, no. 1, pp. 69–76, 2005.

[64] K. Schaaff and T. Schultz, "Towards emotion recognition from electroencephalographic signals," in *Affective Computing and Intelligent Interaction and Workshops, 2009. ACII 2009. 3rd International Conference on*. IEEE, 2009, pp. 1–6.

[65] D. Palomba, A. Angrilli, and A. Mini, "Visual evoked potentials, heart rate responses and memory to emotional pictorial stimuli," *International journal of psychophysiology*, vol. 27, no. 1, pp. 55–67, 1997.

[66] A. Delorme and S. Makeig, "Eeglab: an open source toolbox for analysis of single-trial eeg dynamics including independent component analysis," *Journal of neuroscience methods*, vol. 134, pp. 9–21, 2004.

[67] G. Valenza, A. Greco, C. Gentili, A. Lanata, L. Sebastiani, D. Menicucci, A. Gemignani, and E. Scilingo, "Combining electroencephalographic activity and instantaneous heart rate for assessing brain–heart dynamics during visual emotional elicitation in healthy subjects," *Phil. Trans. R. Soc. A*, vol. 374, no. 2067, p. 20150176, 2016.

[68] J. Theiler, "Two tools to test time series data for evidence of chaos and/or nonlinearity," *Integrative physiological and behavioral science*, vol. 29, no. 3, pp. 211–216, 1994.

[69] F. Artoni, C. Chisari, D. Menicucci, C. Fanciullacci, and S. Micera, "Remov: Eeg artifacts removal methods during lokomat lower-limb rehabilitation," in *Biomedical robotics and biomechatronics (BioRob), 2012 4th IEEE RAS & EMBS international conference on*. IEEE, 2012, pp. 992–997.

[70] P. D. Welch, "The use of fast fourier transform for the estimation of power spectra: A method based on time averaging over short, modified periodograms," *IEEE Transactions on audio and electroacoustics*, vol. 15, no. 2, pp. 70–73, 1967.

[71] F. Mormann, K. Lehnertz, P. David, and C. E. Elger, "Mean phase coherence as a measure for phase synchronization and its application to the eeg of epilepsy patients," *Physica D: Nonlinear Phenomena*, vol. 144, no. 3-4, pp. 358–369, 2000.
[72] S. Holm, "A simple sequentially rejective multiple test procedure," *Scandinavian journal of statistics*, pp. 65–70, 1979.
[73] S. A. Alchamlat and F. Farnir, "Knn-mdr: a learning approach for improving interactions mapping performances in genome wide association studies," *BMC bioinformatics*, vol. 18, no. 1, p. 184, 2017.
[74] N. Suguna and K. Thanushkodi, "An improved k-nearest neighbor classification using genetic algorithm," *International Journal of Computer Science Issues*, vol. 7, no. 2, pp. 18–21, 2010.
[75] A. Greco, S. M. Benvenuti, C. Gentili, D. Palomba, E. P. Scilingo, and G. Valenza, "Assessment of linear and nonlinear/complex heartbeat dynamics in subclinical depression (dysphoria)," *Physiological measurement*, vol. 39, no. 3, p. 034004, 2018.
[76] N. Mukhtar, M. A. Khan, and N. Chiragh, "Effective use of evaluation measures for the validation of best classifier in urdu sentiment analysis," *Cognitive Computation*, vol. 9, no. 4, pp. 446–456, 2017.
[77] J. M. Ver Hoef and H. Temesgen, "A comparison of the spatial linear model to nearest neighbor (k-nn) methods for forestry applications," *PloS one*, vol. 8, no. 3, p. e59129, 2013.
[78] M. Aci, C. İnan, and M. Avci, "A hybrid classification method of k nearest neighbor, bayesian methods and genetic algorithm," *Expert Systems with Applications*, vol. 37, no. 7, pp. 5061–5067, 2010.
[79] R. Kohavi and F. Provost, "Glossary of terms," *Machine Learning*, vol. 30, no. June, pp. 271–274, 1998.
[80] Y.-J. Liu, M. Yu, G. Zhao, J. Song, Y. Ge, and Y. Shi, "Real-time movie-induced discrete emotion recognition from eeg signals," *IEEE Transactions on Affective Computing*, no. 1, pp. 1–1, 2017.
[81] S. Ponten, A. Daffertshofer, A. Hillebrand, and C. J. Stam, "The relationship between structural and functional connectivity: graph theoretical analysis of an eeg neural mass model," *Neuroimage*, vol. 52, no. 3, pp. 985–994, 2010.
[82] V. Sakkalis, "Review of advanced techniques for the estimation of brain connectivity measured with eeg/meg," *Computers in biology and medicine*, vol. 41, no. 12, pp. 1110–1117, 2011.
[83] G. Valenza, A. Greco, M. Bianchi, M. Nardelli, S. Rossi, and E. P. Scilingo, "Eeg oscillations during caress-like affective haptic elicitation," *Psychophysiology*, p. e13199, 2018.
[84] B. Horwitz, "The elusive concept of brain connectivity," *Neuroimage*, vol. 19, no. 2, pp. 466–470, 2003.
[85] A. Von Stein and J. Sarnthein, "Different frequencies for different scales of cortical integration: from local gamma to long range alpha/theta synchronization," *International journal of psychophysiology*, vol. 38, no. 3, pp. 301–313, 2000.
[86] A. Bruns and R. Eckhorn, "Task-related coupling from high-to low-frequency signals among visual cortical areas in human subdural recordings," *International journal of psychophysiology*, vol. 51, no. 2, pp. 97–116, 2004.
[87] A. Gabriel and R. Eckhorn, "A multi-channel correlation method detects traveling γ-waves in monkey visual cortex," *Journal of neuroscience methods*, vol. 131, no. 1, pp. 171–184, 2003.
[88] S. Weiss and P. Rappelsberger, "Long-range eeg synchronization during word encoding correlates with successful memory performance," *Cognitive Brain Research*, vol. 9, no. 3, pp. 299–312, 2000.
[89] L. Aftanas, A. Varlamov, S. Pavlov, V. Makhnev, and N. Reva, "Affective picture processing: event-related synchronization within individually defined human theta band is modulated by valence dimension." *Neuroscience Letters*, vol. 303, no. 2, pp. 115 – 118, 2001.
[90] G. Knyazev, J. Slobodskoj-Plusnin, and A. Bocharov, "Event-related delta and theta synchronization during explicit and implicit emotion processing," *Neuroscience*, vol. 164, no. 4, pp. 1588 – 1600, 2009.
[91] E. K. Silberman and H. Weingartner, "Hemispheric lateralization of functions related to emotion," *Brain and cognition*, vol. 5, no. 3, pp. 322–353, 1986.
[92] D. M. Tucker, "Lateral brain function, emotion, and conceptualization." *Psychological bulletin*, vol. 89, no. 1, p. 19, 1981.
[93] M. M. Muller, A. Keil, T. Gruber, and T. Elbert, "Processing of affective pictures modulates right-hemispheric gamma band eeg activity," *Clinical Neurophysiology*, vol. 110, no. 11, pp. 1913 – 1920, 1999.
[94] J.-P. Royet, D. Zald, R. Versace, N. Costes, F. Lavenne, O. Koenig, and R. Gervais, "Emotional responses to pleasant and unpleasant olfactory, visual, and auditory stimuli: a positron emission tomography study," *The Journal of Neuroscience*, vol. 20, no. 20, pp. 7752–7759, 2000.
[95] T. D. Wager, K. L. Phan, I. Liberzon, and S. F. Taylor, "Valence, gender, and lateralization of functional brain anatomy in emotion: a meta-analysis of findings from neuroimaging," *Neuroimage*, vol. 19, no. 3, pp. 513–531, 2003.
[96] S. Fitzgibbon, K. Pope, L. Mackenzie, C. Clark, and J. Willoughby, "Cognitive tasks augment gamma eeg power," *Clinical Neurophysiology*, vol. 115, no. 8, pp. 1802 – 1809, 2004.
[97] B. W. McMenamin, A. J. Shackman, J. S. Maxwell, D. R. Bachhuber, A. M. Koppenhaver, L. L. Greischar, and R. J. Davidson, "Validation of ica-based myogenic artifact correction for scalp and source-localized eeg," *NeuroImage*, vol. 49, no. 3, pp. 2416 – 2432, 2010.
[98] C. Feng, W. Li, T. Tian, Y. Luo, R. Gu, C. Zhou, and Y.-j. Luo, "Arousal modulates valence effects on both early and late stages of affective picture processing in a passive viewing task," *Social neuroscience*, vol. 9, no. 4, pp. 364–377, 2014.

Alberto Greco (S12-M16), Ph.D., graduated in Biomedical Engineering from the University of Pisa (Italy), in 2010. He received a PhD degree in Automatics, Robotics and Bioengineering from University of Pisa in 2015. He is currently research fellow at Research Center "E. Piaggio", University of Pisa and he was a visiting fellow at the University of Essex, UK, in 2014. His main research interests are physiological modeling, wearable monitoring system, and biomedical signal processing. Applications include affective computing and the assessment of mood and consciousness disorders. He is author of several international scientific contributions, in these fields, published in peer-reviewed international journals, conference proceedings, and books. He has been involved in several European research projects.

Gaetano Valenza (S10-M12), M.Eng., Ph.D., is currently an Assistant Professor of Bioengineering at the University of Pisa, Pisa, Italy. His research interests include statistical and nonlinear biomedical signal and image processing, cardiovascular and neural modeling, and wearable systems for physiological monitoring. Applications of his research include the assessment of autonomic nervous system activity on cardiovascular control, brain-heart interactions, affective computing, assessment of mood and mental/neurological disorders. He is author of more than 100 international scientific contributions in these fields. He has been involved in several international research projects, and currently is the scientific co-coordinator of the European collaborative project H2020-PHC-2015-689691-NEVERMIND. Dr. Valenza has been member of the editorial board/guest editor of several international scientific journals.

Enzo Pasquale Scilingo (M10), PhD, is an Associate Professor in Electronic and Information Bioengineering at the University of Pisa. He has several teaching activities and he is supervisor of several PhD students. He coordinated a European project EC-FP7-ICT-247777 "PSYCHE-Personalised monitoring SYstems for Care in mental Health", and he is currently coordinating the European project H2020-PHC-2015-689691 NEVERMIND - NEurobehavioural predictiVE and peRsonalised Modelling of depressIve symptoms duriNg primary somatic Diseases with ICT-enabled self-management procedures. His main research interests are in wearable monitoring systems, human-computer interfaces, biomedical and biomechanical signal processing, modeling, control and instrumentation. He is author of more than 150 papers on peer-review journals, contributions to international conferences and chapters in international books.